

See discussions, stats, and author profiles for this publication at: <https://www.researchgate.net/publication/272128727>

Femtosecond Pump–Push–Probe and Pump–Dump–Probe Spectroscopy of Conjugated Polymers: New Insight and Opportunities

ARTICLE *in* JOURNAL OF PHYSICAL CHEMISTRY LETTERS · SEPTEMBER 2014

Impact Factor: 7.46 · DOI: 10.1021/jz501549h

CITATIONS

4

READS

48

1 AUTHOR:



Tak W Kee

University of Adelaide

44 PUBLICATIONS 1,277 CITATIONS

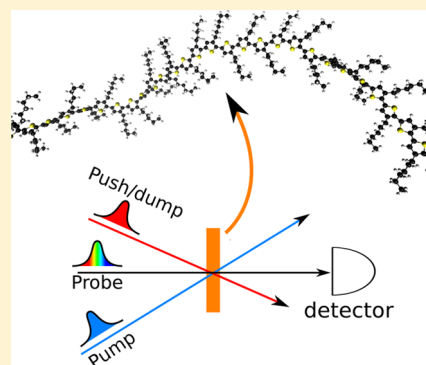
SEE PROFILE

Femtosecond Pump–Push–Probe and Pump–Dump–Probe Spectroscopy of Conjugated Polymers: New Insight and Opportunities

Tak W. Kee*

Department of Chemistry, The University of Adelaide, Adelaide, South Australia 5005, Australia

ABSTRACT: Conjugated polymers are an important class of soft materials that exhibit a wide range of applications. The excited states of conjugated polymers, often referred to as excitons, can either deactivate to yield the ground state or dissociate in the presence of an electron acceptor to form charge carriers. These interesting properties give rise to their luminescence and the photovoltaic effect. Femtosecond spectroscopy is a crucial tool for studying conjugated polymers. Recently, more elaborate experimental configurations utilizing three optical pulses, namely, pump–push–probe and pump–dump–probe, have been employed to investigate the properties of excitons and charge-transfer states of conjugated polymers. These studies have revealed new insight into femtosecond torsional relaxation and detrapping of bound charge pairs of conjugated polymers. This Perspective highlights (1) the recent achievements by several research groups in using pump–push–probe and pump–dump–probe spectroscopy to study conjugated polymers and (2) future opportunities and potential challenges of these techniques.



Conjugated polymers are organic semiconducting materials that exhibit light-emitting and photovoltaic effects. Today, significant progress has been made in the synthesis of conjugated polymers to produce a large number of materials with a wide range of absorption and emission wavelengths.^{1–15} Recently, conjugated polymers with absorption and emission in the red or near-infrared spectral regions were reported and are termed low-band-gap conjugated polymers.^{1,8,13} Currently, these polymers produce some of the highest power conversion efficiencies for conjugated-polymer based solar cells.^{16–18}

Experimental femtosecond configurations utilizing three optical pulses have been employed to investigate the properties of excitons and charge-transfer states of conjugated polymers.

One of the most important applications of conjugated polymers is their function as the light-harvesting materials and electron donors in organic solar cells.^{13,18–24} Electron acceptors including the fullerene derivatives PC₆₀BM, PC₇₀BM, and ICBM are used typically along with conjugated polymers in a solar cell to achieve efficient charge carrier generation. Upon photoexcitation, energy is initially deposited in the chromophoric units with a high Franck–Condon factor as excitons. Subsequently, relaxation occurs in the nuclear degrees of freedom in the excited electronic states, including planarization of monomeric units and vibrational relaxation, to enable

excitons to undergo self-trapping by lowering their energy.^{25–30} Excitons can migrate to chromophoric units with lower energies to further undergo relaxation, which is often referred to as exciton diffusion or exciton migration. The diffusion length (L_D) of excitons is defined as $L_D = (D\tau)^{1/2}$, where D is the exciton diffusion constant and τ is the exciton lifetime. In the event that the conjugated polymer–electron acceptor interface is within L_D for an exciton, dissociation of the exciton is possible in which an electron is transferred to the acceptor, leaving a “hole” in the conjugated polymer. A portion of the electron and hole pairs are bound across the interface initially, forming charge-transfer states, which may either undergo geminate recombination or dissociation to form charge carriers. Recently, significant progress has been made to understand charge carrier generation at early time.^{31–38} Within 40 fs of excitation, the electron–hole separation is estimated to be ~ 4 nm.³⁵ It was reported that charge separation occurs through access to delocalized π -electron states in the ordered regions of the fullerene acceptor material.

Femtosecond laser spectroscopic techniques, including pump–probe spectroscopy and fluorescence upconversion spectroscopy, have been indispensable tools in understanding the behavior of excitons in terms of their migration and dissociation to form charge carriers.^{39–43} In femtosecond pump–probe spectroscopy, the pump pulse excites the system under investigation, and the probe pulse detects the effect of the pump-induced excitation. By modulating the pump pulse

Received: July 23, 2014

Accepted: September 3, 2014

Published: September 3, 2014



and optically delaying the probe pulse relative to the pump pulse, the change in optical density (ΔOD) is measured as a function of time. Recently, elaborate femtosecond spectroscopic configurations utilizing a secondary perturbation pulse including pump–push–probe,^{31,44,45} pump–push–photocurrent,³¹ and pump–dump–probe spectroscopy^{25,46} have been used to provide further insight into the behavior of conjugated polymer excitons. Many of these techniques have been applied previously to study the early ground-state intermediate and stimulated emission (SE) of the cyanobacterial phytochrome Cph1.^{47,48} While pump–probe spectroscopy monitors the evolution of the excited-state species, pump–push–probe and pump–dump–probe techniques offer the opportunity to control the evolution of the excited-state species by either further excitation to a higher-energy electronic state or stimulated deactivation to the ground electronic state. The ability to control the evolution of the excited-state species has led to substantial progress in the research of conjugated polymers.^{25,31,44–46} The progress thus far was possible owing to the availability of highly stable laser sources, which initially led to significant improvements in the sensitivity of pump–probe spectroscopy (ΔOD). These improvements in turn made it possible to resolve the effect of secondary perturbations ($\Delta\Delta OD$), which is inherently noisier than the ΔOD signals. To date, studies utilizing these techniques have revealed the nature of charge-transfer states,³¹ torsional relaxation,^{25,44} high-energy excitons of conjugated polymers and oligomers.^{44,45} In this Perspective, a summary of recent advances is provided. In addition, future opportunities and challenges of the applications of these multipulse techniques with a secondary perturbation pulse will be outlined.

Pump–Push–Probe Spectroscopy. Conjugated polymers were investigated using the pump–push–probe technique in 2002. Gadermaier et al. used this technique to study methyl-substituted ladder-type poly(*para*)phenyl.⁴⁹ In this work, the pump pulse excites the conjugated polymer to generate singlet excitons. The push pulse arrives at <3 ps after the pump pulse to further excite these excitons.⁴⁹ These authors reported that the push pulse promotes the excitons to a high-energy state in which excitons are dissociated to yield charge carriers with a 7% efficiency. This work demonstrated the feasibility of the pump–push–probe technique for studying conjugated polymers.

Figure 1A shows the schematic diagram of pump–push–probe spectroscopy. The pump and push pulses are modulated at frequencies ω and $\omega/2$, respectively, to produce a signal that is specific to the effect of the pump–push-induced excitation. In addition to probing a change in the optical density due to the pump–push excitation, a photocurrent signal can be detected as well, as shown in Figure 1B. An energy diagram showing the photophysical processes involving the pump, push, and probe pulses is given in Figure 1C. The pump pulse excites the conjugated polymer to the S_1^* state, which has a significant Franck–Condon overlap with the ground state, S_0 . The push pulse arrives at the conjugated polymer with a time delay of $\tau \geq 0$ to further excite the S_1 state to states with a higher energy, S_n . Although further excitation by the push pulse is shown to occur in the S_1 state, it is also possible for the push pulse to further excite other transient species including charge-transfer states and free carriers. For instance, using a probe pulse with a wavelength resonant to the S_1 – S_n transition, one can monitor the effect of the push pulse on the population of the S_1 state. Alternatively, in a pump–push–photocurrent measurement,³¹ the effect of the push pulse on the generated photocurrent is

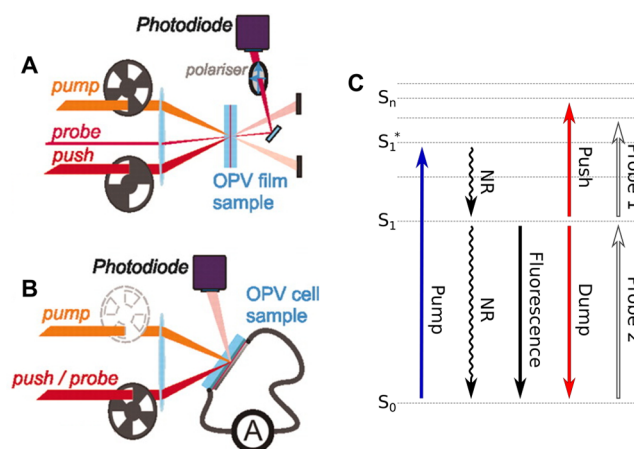


Figure 1. Schematic diagrams of the (A) pump–push–probe and (B) pump–push photocurrent experiments of an OPV sample. Reprinted with permission from ref 31, copyright 2012, AAAS. Note that the push pulse is replaced with a dump pulse in the pump–dump–probe experiment. (C) An energy diagram showing the photophysical processes involved in the experiment. Note that intersystem crossing is not shown, and the push or dump pulse is only present in the three-pulse experiment.

recorded as a function of the pump–push delay time. The enhancement in the generated photocurrent can then be recorded.

In a report by Bakulin et al. in 2012,³¹ femtosecond pump–push–probe and pump–push–photocurrent techniques were used to investigate organic photovoltaic (OPV) cells composed of a number of conjugated polymers. This study aimed at addressing the dynamics of the electron–hole pairs that are still localized at the interface. As mentioned earlier, in the exciton dissociation process, the exciton undergoes a charge-transfer reaction at the donor–acceptor interface. In doing so, the electron and hole must overcome the mutual Coulomb attraction that binds the singlet exciton. The charge-transfer step is driven by offset energy levels across the donor–acceptor interface. The electron and hole maintain their electrostatic attraction across the interface, forming a charge-transfer state. In the pump–push–photocurrent scheme, Bakulin et al. used a pump at 580 nm (above the band gap of the conjugated polymers) and a push at 2200 nm. The resultant increase in photocurrent, which is expressed as a percentage increase, as a function of the pump–push delay, is shown in Figure 2A. It is remarkable that the level of increase in photocurrent in the conjugated polymer OPVs is as high as 40%. This work clearly demonstrated the presence of charges as charge-transfer states in some of the OPVs. By promoting the charge-transfer states to an excited state of similar characteristics, the electrostatically bound electron–hole pairs are given a new opportunity to undergo charge separation. Figure 2B shows the pump–push–probe transient absorption results of one of the conjugated polymer OPVs in which the probe wavelength is 3 μm . It is clear that the push pulse has a significant effect in exciting the charge-transfer state, which manifests as a transient absorption bleach signal. It is interesting that the push-induced increase in photocurrent is dependent on the donor and acceptor pair. For instance, the relative increase is higher for the OPV composed of PFB/F8BT than that of P3HT/PC₆₀BM. In this case, an important factor is the external quantum efficiency (EQE) of the OPV. The donor–acceptors with a low EQE (e.g., PFB/F8BT) have a high amount of bound charges and hence

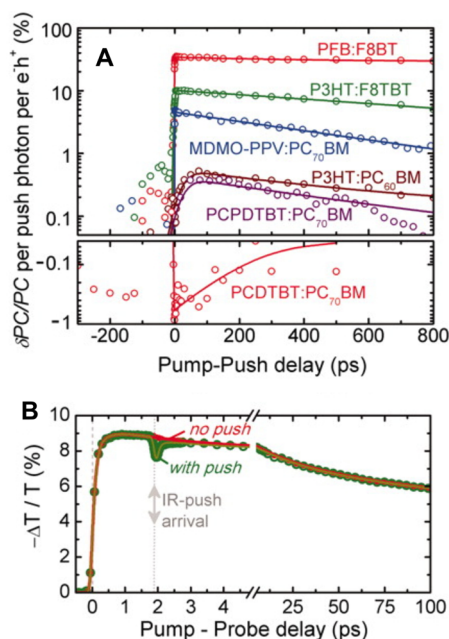


Figure 2. (A) The results of a pump–push photocurrent experiment on a set of OPVs under above-band-gap excitation (580 nm). The push-induced increase in photocurrent is as high as 40%. (B) Transient absorption kinetics for MDMO-PPV/PC₇₀BM film excited at 580 nm and probed at 3 μ m. The green line shows dynamics with the push pulse (2200 nm) arriving at ~ 2 ps delay. Reprinted with permission from ref 31, copyright 2012, AAAS.

produce a significant relative increase in photocurrent. For an efficient photoconversion system, the push-induced photocurrent is low due to a low level of bound charges. Bakulin et al. also performed atomistic “many-body” modeling to demonstrate that the electron–hole separation is noticeably longer in the excited charge-transfer state than that in the lowest-lying charge-transfer state. This result is consistent with decoupling of the electron–hole pair as a result of promotion of the charge-transfer state to an excited charge-transfer state. In short, this work revealed that the driving energy of charge separation in OPVs is the energy that is required for charges to reach the delocalized band states. Even though these states are very short-lived (<1 ps), they offer the charges the ability to overcome the dominant Coulomb attraction to achieve large-scale charge separation.

In a separate study by Clark et al., femtosecond pump–push–probe spectroscopy was used to investigate rapid torsional relaxation of a series of oligofluorenes.⁴⁴ In this study, a pump pulse centered at 390 nm was used to excite the oligofluorenes to the S_1 state, and a push pulse of 780 nm was used to promote the S_1 state to a high-energy excited state, S_n . The SE and excited-state absorption of the oligofluorenes were probed within the range of 460–520 nm. In addition to the S_1 and S_n states, Clark et al. also examined the state S_m of the oligofluorenes, which is a localized B_u state and was accessed by a direct photoexcitation at 260 nm. First, the wave function delocalization in each of these states was examined. Unsurprisingly, the results show that the S_1 and S_n states have a substantial level of delocalization. However, the electron and hole pair of the S_m state is confined to a single phenyl ring in the oligofluorenes.⁴⁴ Next, the pump–push–probe results were compared with the pump–probe results to demonstrate the effect of the push pulse. In the pump–probe results, the SE

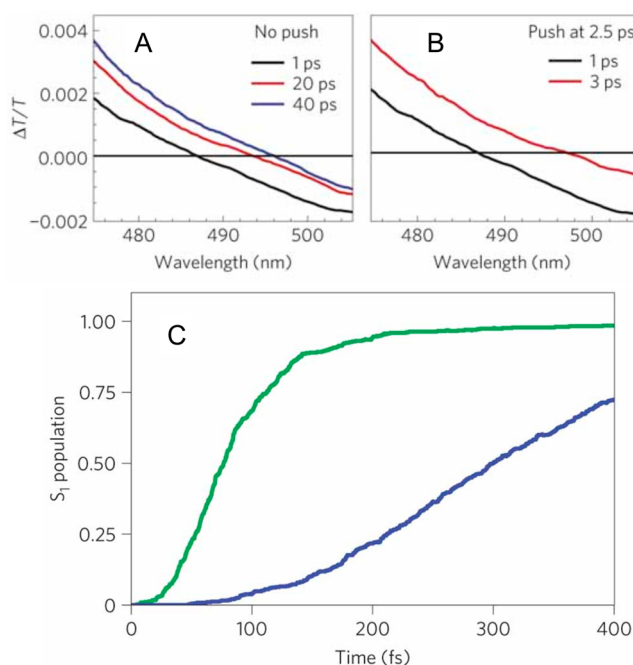


Figure 3. (A) Pump–probe and (B) pump–push–probe spectra of a pentamer oligofluorene at the zero-crossing region. Note the slow red shift in the pump–probe spectra. The order of the spectra in (A) from bottom to top is 1, 20, and 40 ps. The spectra in (B) show that the push pulse (arriving at 2.5 ps) causes a rapid red shift. (C) An increase of population of the S_1 state during nonadiabatic dynamics starting from the S_m (blue) and S_n (green) states, which are prepared by a UV pump pulse and a visible pump and a near-IR push pulse, respectively. The population of S_n quickly drops to S_1 within ~ 100 fs, showing ultrafast nonadiabatic relaxation, whereas S_m relaxes on a much longer time scale (>400 fs). Reprinted with permission from Macmillan Publishers Ltd: Nature Physics (ref 44), copyright 2012.

band of the pentamer fluorene exhibits a slow red shift over 40 ps, as shown in Figure 3A. Interestingly, in the presence of the push pulse, arriving at 2.5 ps after the pump pulse, the SE band shows a rapid red shift, as shown in Figure 3B. Using optical pulses with an instrument response function of ≤ 20 fs, the time constant of this rapid red shift was shown to be ~ 60 fs. The results indicate that upon the push-induced excitation of the S_1 to S_n state, ultrafast relaxation from the S_n state back to the S_1 state occurs, resulting in a red shift with a time constant of ~ 60 fs.

To reveal further insight into the S_n – S_1 transition, nonadiabatic excited-state molecular dynamics was used to simulate the process. One of the most informative results is the population recovery of the S_1 state after the S_1 – S_n transition induced by the push pulse, which is shown in Figure 3C. The S_n state undergoes internal conversion within 100 fs to populate the S_1 state (green curve in Figure 3C). Clark et al. further argued that the ultrafast internal conversion occurs for the following two reasons. First, the internal conversion involves a large number of intermediate states between S_n and S_1 . These states have similar exciton delocalization to that of S_n . As a result, significant nonadiabatic couplings between states enable the fast S_n to S_1 transition. Second, the potential energy surfaces of delocalized states including S_n are relatively steep along the torsional mode and the C=C stretching mode. In this case, the wavepacket involved in the relaxation can gain substantial kinetic energy along these two vibrational coordinates, converting the excess electronic energy to vibrations. The

behavior of the ultrafast torsional relaxation is highly analogous to inertial solvation dynamics,^{50–52} in which excess electronic energy of the solute is transferred to the surrounding solvent molecules by inertial solvent motions. In the case of oligofluorenes, the excess electronic energy is dumped into the torsional modes, enabling the nuclei to move in a quasi-independent fashion to the solvent environment. In contrast, the S_m – S_1 transition occurs relatively slowly, as shown in Figure 3C (blue curve). The slower rate is due to the relatively flat potential energy surfaces of S_m , as well as fewer transitions between S_m and S_1 . In this case, the wavepacket reaches the S_1 state with a significantly lower kinetic energy. In short, pump–push–probe spectroscopy was used in this study to reveal ultrafast torsional relaxation in oligofluorenes. This study contributes significantly to the understanding of couplings between the electronic and nuclear degrees of freedom in conjugated systems.

In 2014, Tapping and Kee reported charge carrier generation by optical pumping of poly(3-hexylthiophene) (P3HT) singlet excitons.⁴⁵ They used pump–push–probe spectroscopy to demonstrate that photoexcitation of P3HT singlet excitons to high-energy excitonic states leads to a signal consistent with rapid geminate recombination of the generated charges. In their study, a pump with a wavelength of 400 nm, a push of either 900 nm or 1200 nm, and a probe of 1050 nm were used. In the experimental scheme, the 400 nm pump arrives at $t = 0$ ps to excite P3HT from the ground state (S_0) to the singlet excited state with a large Franck–Condon factor (S_1^*). This excited state undergoes nonradiative relaxation in the forms of planarization of monomeric units and exciton self-trapping to yield the equilibrated singlet excited state (S_1) in <20 ps.^{25–30} The push pulse arrives ~25 ps after the pump pulse to further excite the S_1 state to a high-energy excitonic state, S_n . The probe pulse records the effect of the pump and push pulses by monitoring the S_1 – S_n absorption (Figure 1C), which centers at around 1050 nm.

The blue curve in Figure 4A shows the transient absorption signal at 1050 nm. This signal exhibits decay time constants of 135 and 530 ps (extracted from data with a time window of 2.5 ns), which were assigned to slow torsional relaxation and the exciton lifetime of P3HT, respectively.⁴⁵ The red curve in Figure 4A shows the transient absorption signal in the presence of the push pulse. The push pulse induces an absorption bleach at $t \approx 25$ ps. The majority of the transient absorption signal exhibits a rapid recovery due to the fast S_n – S_1 state relaxation. However, a portion of the signal shows an incomplete recovery.

To probe the push-induced dynamics with a high sensitivity, an experiment in which the push pulse is modulated while keeping the pump pulse on continuously was conducted. This measurement yielded the difference between ΔOD with the push pulse on and that with the push pulse off. The $\Delta\Delta OD$ results are shown in Figure 4B. First, the “missing” signal owing to the incomplete recovery in Figure 4A manifests as a $\Delta\Delta OD$ signal with long recovery time constants, and it accounts for 11% of the total signal. It mirrors the ΔOD signal with long decay time constants. As such, the time constants of this $\Delta\Delta OD$ signal component are fixed at 135 and 530 ps during data analysis. Tapping and Kee argued that the “missing” excitons owing to the push-pulse-induced excitation are attributable to exciton dissociation to generate charge carriers in P3HT, which has been observed in a different conjugated polymer.⁴⁹ The resultant charge carriers, which reside on a single P3HT chain, are able to undergo rapid geminate

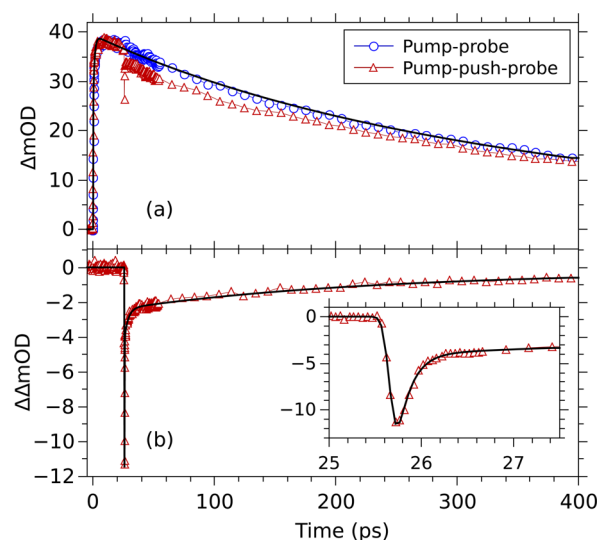


Figure 4. (A) The dynamics of the exciton-induced absorption at 1050 nm in the pump–probe (blue circles) and pump–push–probe experiments (red triangles). The pump and push wavelengths are 400 and 900 nm, respectively. (B) The change in ΔOD ($\Delta\Delta OD$) due to the push pulse. Fit curves are indicated as solid black curves. Reprinted with permission from ref 45.

recombination to yield ground-state P3HT. This result is supported by a push-pulse-induced, positive $\Delta\Delta OD$ signal in the ground-state absorption region.⁴⁵ In addition to the long recovery time constants, the $\Delta\Delta OD$ signal shows a rapid recovery in the dynamics, which consists of two short time constants of 0.16 and 2.4 ps. The amplitudes of the $\Delta\Delta OD$ signal with these two time constants account for 89% of the total signal amplitude. The short time constant of 0.16 ps is consistent with the time scale of femtosecond torsional relaxation reported by Clark et al.,⁴⁴ as highlighted in an earlier part of this Perspective. The time constant of 2.4 ps is attributable to larger amplitude and further torsional relaxation, which has been observed in previous studies.^{25,30} In short, Tapping and Kee used pump–push–probe spectroscopy to investigate the high-energy excitonic states above the singlet exciton level. They demonstrated that promotion of the singlet exciton to this level results in charge carrier generation with a yield of 11%, indicating that the high-energy excitonic states are highly delocalized. The highly delocalized states have sufficient energy to overcome the mutual Coulomb attraction between the electron and hole pair to generate charge carriers.

Pump–Dump–Probe Spectroscopy. Femtosecond pump–dump–probe spectroscopy was used in the 1990s to investigate molecular isomerization in a controlled fashion.⁵³ In addition, Gai et al. used this technique to investigate bacteriorhodopsin and revealed the presence of a near-infrared excited-state absorption band.⁵⁴ Thereafter, pump–dump–probe spectroscopy has been used to study not only conjugated polymers^{25,46} but also pigments including β -carotene and protein chromophores.^{55,56} Figure 1A also shows the schematic diagram of the pump–dump–probe experiment, whereby the push pulse is replaced by a dump pulse. An energy diagram highlighting the photophysical processes involved in a pump–dump–probe experiment is shown in Figure 1C. The dump pulse has a wavelength that falls under the fluorescence spectrum of the system under investigation, thereby deactivating the excited-state population to a nonequilibrium ground state (NGS) by

stimulated transition. By monitoring the evolution of the SE and the NGS after the arrival of the dump pulse, the effects of the dump pulse can be recorded.

In 2011, Busby et al. reported the use of pump–dump–probe spectroscopy to study excited-state self-trapping and ground-state relaxation in P3HT.²⁵ In this study, a pump wavelength of 400 nm, a dump of 600 nm, and probe ranging from 380 to 700 nm were used. P3HT was studied in solution at low concentration under the isolated chain condition to avoid contributions from interchain interactions. First, these authors performed pump–probe experiments on P3HT, in which the results show a red shift in the SE band and a blue shift in the ground-state bleach (GSB) signal. The red shift in SE is attributable to both intrachain excitonic energy transfer (EET) and excited-state self-trapping. To differentiate these two processes, the authors turned to the blue-shifting GSB. They argued that in the case of EET, the excitation and GSB signal should migrate toward the low-energy and red-absorbing regions of the polymer. This excitation migration induces a red shift in both the SE and GSB signal, as is observed commonly in the relaxation dynamics of multichromophore photosynthetic complexes.⁵⁷ However, a blue-shift in the GSB of P3HT, that is, a lack of red shift, was observed. As a consequence, the authors argued that excited-state self-trapping is the most likely process for the red shift observed in the SE band, as opposed to EET. While EET cannot be excluded completely, the evidence of its significant contribution is absent.

Next, Busby et al. turned to pump–dump–probe spectroscopy to gain further insight into the blue-shifting GSB. While the pump generates an exciton population, the dump pulse halts the evolution of the exciton population by transferring it to the ground electronic state, or NGS. The key advantage of pump–dump–probe spectroscopy in this study is its ability to track the evolution of NGS to give important details on the structural and electronic configurations of P3HT. The $\Delta\Delta\text{OD}$ data are shown in Figure 5A. First, the pump–dump–probe SE also exhibits a red shift, which is identical to the pump–probe SE. The NGS signal, however, which manifests as a blue-shifting signal from 2.4 to 2.8 eV, indicates that the initially formed ground state is red-shifted (~ 2.4 eV) relative to the thermally equilibrated ground state (2.74 eV). This state further blue shifts to form the equilibrated ground state.

The NGS and SE peak shifts were compared using a normalized peak shift function $S(t)$. The $S(t)$ for SE and NGS at various dump times are shown in Figure 5B, outlining the different decay kinetics of $S(t)$ for these processes. It is clear from Figure 5B that excited-state self-trapping, as indicated by the $S(t)$ for SE, occurs significantly faster than the torsional relaxation in the ground state, as represented by the $S(t)$ for NGS. Furthermore, the kinetics of the NGS blue shift exhibit a dependence on dump time as shown in Figure 5B. The slow component of the kinetics becomes more prominent as the dump time increases, indicating population recovery from large-scale molecular motions in the excited state, that is, planarization of monomeric units. While it is well-known that this type of molecular motion occurs in the excited state of P3HT, the population that is dumped to the ground electronic state has inter-ring bonds that have a single-bond character and are free to undergo torsional motions. The photophysical processes of P3HT in the pump–dump excitation scheme are shown in Figure 5C. Photoexcitation induces the double bonds on the P3HT chain to undergo rearrangement to form a quinoidal structure (Figure 5C-1). These newly rearranged

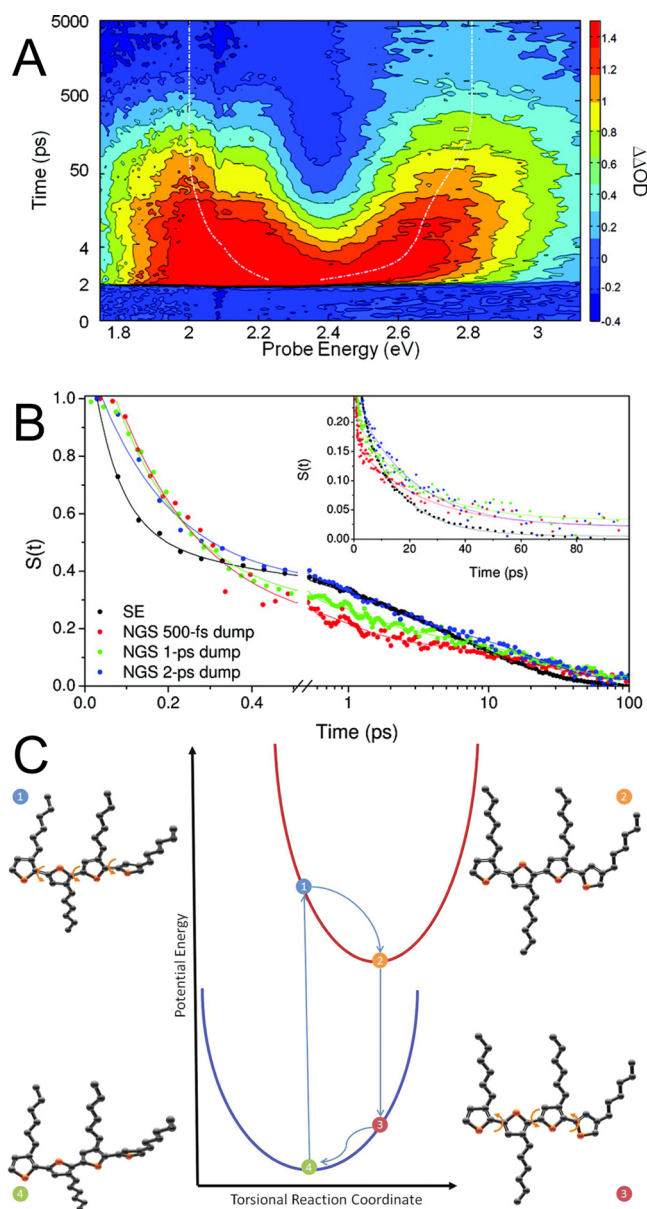


Figure 5. (A) Time- and frequency-resolved $\Delta\Delta\text{OD}$ of RR-P3HT. The dump time is 2 ps. The time is in picoseconds after the dump pulse. Depletions of GSB (2.53 eV) and SE (1.8 eV–2.4 eV) are resolved. The blue shifting of the NGS and the red shifting of the SE bands are highlighted. The excitation energy is 3.1 eV. (B) The $S(t)$ for SE (black) and NGS with a 500 fs (red), 1 ps (green), and 2 ps (blue) dump time. (C) An energy diagram showing the excited-state self-trapping (1 \rightarrow 2) and ground-state torsional relaxation (3 \rightarrow 4) processes. Photoexcitation promotes the equilibrium ground state (4) to the excited electronic state (1), which is accompanied by double bond rearrangement. The excited electronic state (1) then undergoes excited-state self-trapping by planarization to yield the lowest-lying excited electronic state (2). The state (2) is depleted by SE to give a planar NGS (3), which is able to relax to form the equilibrium ground state (4). The torsional motions involved in this photophysical scheme are highlighted with orange arrows. Reprinted with permission from ref 25.

double bonds in turn induce planarization of the thiophene rings to reduce the π -bond angular strain (Figure 5C-2). The dump pulse deactivates the population of the excited electronic state to the ground electronic state, in which the inter-ring bonds are more single bond in character. As a result, the

thiophene rings are no longer constrained to be planar (Figure 5C-3). The P3HT chain then is able to undergo relaxation to return to the nonplanar equilibrium structure (Figure 5C-4). In short, Busby et al. used pump–dump–probe spectroscopy to reveal that excited-state self-trapping occurs substantially faster than torsional relaxation in the ground state. This study has contributed to the understanding of the behavior of excitons in P3HT.

In 2004, Gaab and Bardeen reported anomalous exciton diffusion in the conjugated polymer MEH-PPV using results obtained by pump–dump–probe spectroscopy.⁴⁶ In their study, a pump of 400 nm and a dump and a probe of 600 nm were used. A thin-film sample of MEH-PPV was first excited using a circularly polarized pump. After a certain pump–dump waiting time T_{12} , which ranged from 1 to 42 ps, the linearly polarized dump pulse arrived at the sample to deactivate the excitons with their dipoles aligned with the dump polarization from the excited to the ground electronic states, leaving behind a polarization hole. The probe, with a polarization either parallel or perpendicular to the dump polarization, arrived with a delay time T_{23} relative to the dump pulse to monitor the recovery of the polarized hole, owing to exciton diffusion. The polarization anisotropy decay, which is dependent on the probed signals in both polarizations, can be used to monitor the exciton diffusion process. Figure 6A shows

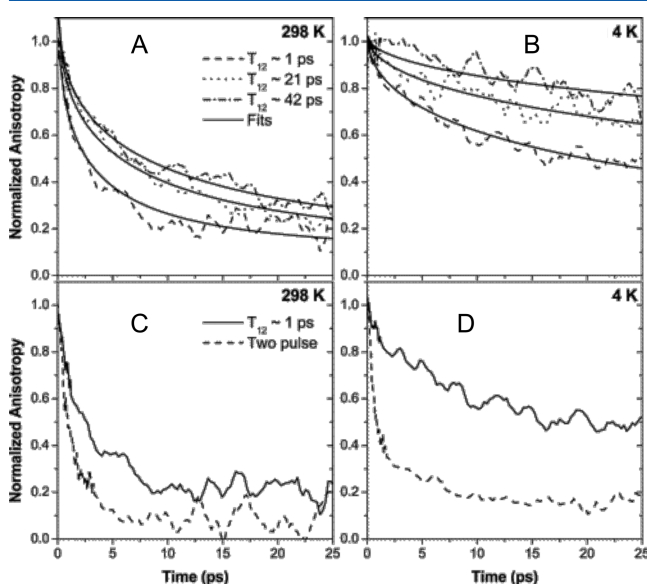


Figure 6. Normalized three-pulse anisotropy decays of a MEH-PPV thin film at (A) 298 and (B) 4 K for pump–dump decays of ~ 1 (dash), ~ 21 (dot), and ~ 42 ps (dot–dash) and the corresponding fits (solid). Normalized three-pulse anisotropy decays at (C) 298 and (D) 4 K for a pump–dump delay of ~ 1 ps (solid) compared with the normalized two-pulse 400–600 pump–probe anisotropy decays. Reprinted with permission from ref 46.

the polarization anisotropy decay as a function of temperature and T_{12} . First, it is clear that the dynamics of the anisotropy decay become slower as T_{12} increases. This result indicates the presence of anomalous exciton diffusion, whereby a time-dependent slowing down of exciton diffusion takes place. Under this condition, exciton diffusion is no longer well-described by the equation $L_D = (D\tau)^{1/2}$. Furthermore, the evidence for anomalous exciton diffusion is clearer at low temperature (4 K), at which the time-dependent slowing down

of exciton diffusion is more pronounced, as shown in Figure 6B. The pump–probe (two-pulse) anisotropy decay shows slower dynamics than the pump–dump–probe anisotropy decay with a T_{12} of 1 ps, as shown in Figure 6C and D. The two sets of results were expected to show agreement as both experiments probed nonequilibrated excitons with similar characteristics. The discrepancy is likely to be related to the photophysical processes that are monitored at the probe wavelength of 600 nm. The presence of an excited-state absorption signal at this wavelength, in addition to SE, has been suggested by previous studies.^{58,59} As a result, the probe monitors at least two different transitions. In the presence of the dump pulse, these transitions are also activated, resulting in transition dipoles of different orientations. The presence of multidirectional transition dipoles in turn results in a rapid anisotropy decay. In contrast, in the pump–probe experiment, where degenerate pump and probe wavelengths (600 nm) were used, the transition is dominated by a single excited state. As a result, the anisotropy decay is unaffected by other transition dipoles. In order to exclude the contribution of ESA, Gaab and Bardeen have suggested the use of pump–dump–upconvert spectroscopy, in which fluorescence upconversion is used to detect solely the time-resolved signals of the exciton. To the author's knowledge, such an experiment has not yet been performed.

Future Opportunities and Potential Challenges. It is interesting that the yield of charge carrier generation of conjugated polymer solar cells is expected to be low considered that the dielectric constants of organic materials are typically only ≤ 4 .⁶⁰ However, some of the recent conjugated polymer solar cells have efficiencies as high as $\sim 10\%$ ⁶¹ and an internal quantum efficiency of $\sim 90\%$.^{35,62,63} Significant progress has been made recently regarding the mechanism by which charge separation occurs in organic solar cells.^{31–38} A recent transient absorption study on organic solar cells prepared with low-band-gap conjugated polymers offered important insight into how charges are generated in these efficient organic solar cells.³⁵ It was reported that charges are able to be separated by ~ 4 nm within 40 fs after photoexcitation. At this distance, the Coulomb attraction between the electron and hole is either at or below thermal energy (room temperature), facilitating efficient charge separation. Moreover, it was also suggested that this ultrafast charge separation occurs through access to delocalized π -electron states in the ordered regions of the fullerene electron acceptor. In addition to electron delocalization, it has been suggested that exciton delocalization plays an important role in efficient organic solar cells.³⁶ Pump–push–probe spectroscopy may be useful in addressing the importance of exciton delocalization and its subsequent dissociation in these solar cells. The combination of pump–push–probe spectroscopy and Monte Carlo simulation will provide insight into delocalization of conjugated polymer excitons. Previously, results obtained from pump–probe anisotropy have yielded important information about conjugated polymer conformations.⁶⁴ In the three-pulse analogue of this measurement, that is, pump–push–probe anisotropy, the level of exciton migration may be deduced, which will provide a qualitative measure of exciton delocalization. In this experiment, the pump pulse excites the conjugated polymer to generate an exciton. The push pulse should then arrive after a long delay time to ensure that the initially prepared exciton is sufficiently relaxed, that is, it occupies a chromophore with a long conjugated length. The probe pulses, with polarizations parallel and

perpendicular to the push pulse, enable the measurement of pump–push–probe anisotropy.

The initial study may be focused on isolated chains. In this case, the pump–push–probe anisotropy experiment can be performed using a “good” solvent in which the conjugated polymer is expected to adopt a random-coil conformation. In analyzing the results, a conjugated polymer chain with a realistic molecular weight (300–1000mers) may be generated using molecular dynamics simulation. For instance, by using a coarse-grained approach to simplify the structure of the polymer and implicit solvent, an equilibrated conformation may be generated within a reasonable time frame. The polymer chain may be divided into chromophoric units based on torsional disorder or chemical defects including the presence of saturated C–C bonds (if any). A Monte Carlo simulation that describes the energy-downhill exciton migration process may be used to study the pump-induced anisotropy by assuming that the excitation energy is initially deposited onto the chromophoric unit with an energy corresponding to the pump photon energy, as demonstrated in previous work.⁶⁴ The simulation may be run for ~20 ps to allow the initially prepared exciton to undergo migration to lower its energy. Typically, a substantial level of exciton migration occurs during the first 20 ps with a significant migration length. Beyond 20 ps, only exciton hopping events with small step sizes are involved. Subsequently, the “trapped” exciton may be artificially moved to another chromophoric unit in the simulation, which mimics the effect of the push pulse, and a second Monte Carlo simulation may be performed to provide insight into the pump–push–probe anisotropy results. The adjustable parameter for achieving a match between simulation and experimental results is the migration length of the “trapped” exciton, which in turn infers the level of delocalization of the exciton as a result of the push-induced excitation. Subsequent studies may be performed on a thin-film sample, which is more relevant to the solar cell applications of conjugated polymers. Monte Carlo simulations of the results can be performed on a simulated polymer thin film with a certain density of exciton traps. By varying the exciton trap density, an agreement between experimental and simulation will be obtained, revealing the level of exciton migration and inferring the level of exciton delocalization.

Thus far, the information on the short-lived and highly delocalized S_n state has been indirect. It is possible that femtosecond stimulated Raman spectroscopy (FSRS),⁶⁵ a technique closely related to pump–push–probe spectroscopy, can offer detailed insight into the characteristics of the S_n state. The FSRS technique, with its ability to acquire Raman spectra with a high resolution in time and spectral domains, presents a significant opportunity to probe the S_n state directly. Recent work by Provencher et al. has demonstrated the application of FSRS for directly probing polaron photogeneration dynamics at polymer–fullerene heterojunctions.³⁴ In this work, an actinic pulse with a duration of 50 fs and a wavelength of 560 nm was used to excite the PCDTBT/PCBM heterojunctions to generate excitons. The evolution of the stimulated Raman spectrum was then probed using a pair of laser pulses. First, a Raman pump pulse that is resonant with the exciton and polaron absorption bands (1.5 ps and 900 nm) was used to excite the transient species to virtual states with resonance enhancement. Then, a short (~50 fs) broad-band pulse was used to generate the excited-state stimulated Raman spectrum of the transient species. The dynamics of the transient species was probed in time by varying the optical delay between the

actinic pulse and the Raman pump and probe pulses. The time-resolved resonance Raman spectra of PCDTBT/PCBM heterojunctions indicate that polarons emerge within 300 fs. Interestingly, further structural evolution on the ≤50 ps time scale is minor, indicating that the polymer conformation hosting the nascent polaron is largely similar to that near equilibrium. This surprising result suggests that charges are free from their mutual Coulomb potential as rich vibrational dynamics associated with charge pair relaxation would be expected otherwise. Although only modest structural evolution is present for polarons, Provencher et al. also studied neat PCDTBT films, and a substantial level of structural evolution was observed for the excitons.³⁴ While these authors presented arguments for intrachain singlet excitons, a highly delocalized exciton in a polymer film should have a large degree of interchain character as well. It is likely that the combination of a higher time resolution (<50 fs) for FSRS and molecular modeling with a higher level of complexity will reveal crucial information about the highly delocalized and short-lived S_n state.

One of the recent developments in the studies of photovoltaics is the use of singlet fission to enhance the power conversion efficiencies of solar cells.^{66,67} Singlet fission is a process in which a singlet excited- and a ground-state molecule ($S_1 + S_0$) share energy to produce a correlated pair of triplet excited molecules (T_1T_1).⁶⁶ Singlet fission has received a significant level of attention recently due to its promise to circumvent the Shockley–Queisser limit, which restricts the power conversion efficiency of a single-junction solar cell to ~32%.⁶⁸ It has been suggested that singlet fission can increase the efficiency limit to 45%.⁶⁹ In addition, a number of solid-state materials, including tetracene, pentacene, 1,3-diphenylisobenzofuran, and zeaxanthin, have exhibited triplet yields well over 100% and mostly close to 200%.⁶⁶ Interestingly, singlet fission has also been suggested in β -carotene and observed in conjugated polymers.^{70,71} Moreover, it was demonstrated recently by Bittner et al. and Rao et al. that an additional advantage of using triplet excitons as the precursors for charges is that the recombination of the triplet charge-separated states is suppressed in organic-fullerene-based bulk-heterojunction photovoltaic cells.^{72,73} While there are significant research activities in the field, the process by which a singlet exciton internally converts to a pair of triplet excitons is still poorly understood. It is possible that pump–push–probe and pump–dump–probe spectroscopy, with their ability to perturb and control dynamic pathways, will be able to offer insight into this potentially critical process. These opportunities are supported by a recent study by Grumstrup et al., in which optical pulse shaping was used to enhance triplet formation in polycrystalline tetracene.⁷⁴ It was shown that an excitation scheme with a number of pulses that are separated in time corresponding to the period of lattice vibrations yielded the highest level of enhancement in the study.⁷⁴ This result suggests that these vibrations control the yield of singlet fission photochemistry. This study also presents the opportunities for using pump–push–probe and/or pump–dump–probe spectroscopy to study singlet fission yields. It is expected that studies on the effects of phase, intensity, and wavelength of the push or dump pulse on the yield of triplet states should offer further understanding of singlet fission.

The potential challenges of pump–push–probe and pump–dump–probe spectroscopy are to perform these experiments using a sufficiently low laser fluence that avoids potential biases

while still providing insight into the investigated processes. As mentioned earlier, pump–push–probe and pump–dump–probe spectroscopy rely on resolving the effect of a secondary perturbation (ΔOD), which is inherently noisier than the ΔOD signals. As a consequence, in order to obtain a reasonable signal-to-noise ratio in experimental data, some of the studies on conjugated polymers and oligomers thus far were performed using a pump laser fluence on the order of $\text{sub-mJ}/\text{cm}^2$.^{25,44,45} Although a relatively high laser fluence was used, it is important to stress that these studies still yielded high-quality results because the samples in these studies were dilute solutions. For thin-film samples, however, the requirement of a low laser fluence is particularly strict because of the presence of exciton–charge and exciton–exciton annihilation reactions.⁷⁵ A previous study by Hodgkiss et al. showed that while exciton–exciton annihilation can be avoided at a fluence of $\sim 30 \mu\text{J}/\text{cm}^2$, exciton–charge annihilation has a lower threshold of $\sim 5 \mu\text{J}/\text{cm}^2$ for a 100 nm P3HT/PCBM blend film.⁷⁵ It is, therefore, very important for researchers in this field to resist the temptation of using a high laser fluence in the quest for a good signal-to-noise ratio in their data. A good example of a pump–push–probe study using an appropriate laser fluence is that by Bakulin et al.³¹ In this study, thin-film samples were examined using a pump fluence of approximately $3 \mu\text{J}/\text{cm}^2$.³¹ Although a push fluence ~ 1000 times greater than that of the pump was used, the lack of any molecular electronic transitions at the push wavelength of 2200 nm relaxes the requirement for a low push fluence. As a result, using a combination of a low-intensity pump pulse and a high-intensity push pulse in this case avoids unwanted effects including exciton–charge annihilation while maintaining a good signal-to-noise ratio for the push-induced effect.

It is very important for researchers in this field to resist the temptation of using a high laser fluence in the quest for a good signal-to-noise ratio in their data.

Summary and Future Outlook. Femtosecond pump–push–probe and pump–dump–probe spectroscopy are emerging as highly useful techniques for revealing underlying photochemistry and photophysics of conjugated polymers. These techniques will be increasingly attractive to many researchers in the field because they only require, in most cases, relatively minor modifications to a femtosecond pump–probe spectrometer. Similar to pump–probe spectroscopy, pump–push–probe and pump–dump–probe spectroscopy use the pump pulse as the primary excitation source. However, a secondary perturbation, the push or dump pulse, is introduced to result in a change in the effect of the pump pulse. The push or dump pulse is able to control the dynamic pathway of the excited state by further exciting or stimulated deactivating the excited state. Thus far, these techniques have been used to study the dissociation of charge-transfer states, dissociation of singlet excitons, excited-state self-trapping, and femtosecond torsional relaxation of conjugated polymers. Significant opportunities lie ahead in the applications of pump–push–probe and pump–dump–probe spectroscopy. These opportunities include further understanding of the highly delocalized excited states of conjugated polymers in terms of the extent of delocalization

and a direct observation of these states by FSRS. Another potential opportunity is to use these techniques to enhance and direct the pathway of singlet fission in molecular crystals or aggregates to generate a pair of correlated triplet states. Finally, owing to an inherently low level of signals in pump–push–probe and pump–dump–probe spectroscopy, a highly stable laser source must be used for future studies. Despite low signal levels, an important requirement for implementing these techniques for future studies of conjugated polymer thin films is to ensure that the pump fluence is below the thresholds for exciton–charge and exciton–exciton annihilation reactions. A low pump fluence will enable probing the real dynamics of the system under investigation without complications from the processes above.

AUTHOR INFORMATION

Corresponding Author

*E-mail: tak.kee@adelaide.edu.au.

Notes

The authors declare no competing financial interest.

Biography

Tak W. Kee leads the Laboratory for Chemical Spectroscopy and Microscopy at the University of Adelaide, Australia. His research aims to develop understanding of fundamental processes in organic solar cells including exciton diffusion and charge carrier generation. Members of his research group use two-pulse and three-pulse femtosecond transient absorption and fluorescence upconversion spectroscopy to investigate conjugated polymers. For further information, visit <http://www.laserchemistry.adelaide.edu.au/Kee/Home.htm>.

ACKNOWLEDGMENTS

The author acknowledges Mr. Patrick C. Tapping for his assistance in preparing this manuscript.

REFERENCES

- (1) Soci, C.; Hwang, I.-W.; Moses, D.; Zhu, Z.; Waller, D.; Gaudiana, R.; Brabec, C. J.; Heeger, A. J. Photoconductivity of a Low-Bandgap Conjugated Polymer. *Adv. Funct. Mater.* **2007**, *17*, 632–636.
- (2) Jin, S. H.; Kang, S. Y.; Kim, M. Y.; Chan, Y. U.; Kim, J. Y.; Lee, K.; Gal, Y. S. Synthesis and Electroluminescence Properties of Poly(9,9-di-*n*-octylfluorenyl-2,7-vinylene) Derivatives for Light-Emitting Display. *Macromolecules* **2003**, *36*, 3841–3847.
- (3) Zou, Y.; Najari, A.; Berrouard, P.; Beaupre, S.; Aich, B. R.; Tao, Y.; Leclerc, M. A Thieno[3,4-*c*]pyrrole-4,6-dione-Based Copolymer for Efficient Solar Cells. *J. Am. Chem. Soc.* **2010**, *132*, 5330–5331.
- (4) Stevens, M. A.; Silva, C.; Russell, D. M.; Friend, R. H. Exciton Dissociation Mechanisms in the Polymeric Semiconductors Poly(9,9-dioctylfluorene) and Poly(9,9-dioctylfluorene-*co*-benzothiadiazole). *Phys. Rev. B* **2001**, *63*, 165213.
- (5) Schwartz, B. J. Conjugated Polymers as Molecular Materials: How Chain Conformation and Film Morphology Influence Energy Transfer and Interchain Interactions. *Annu. Rev. Phys. Chem.* **2003**, *54*, 141–172.
- (6) McCullough, R. D.; Lowe, R. D.; Jayaraman, M.; Anderson, D. L. Design, Synthesis, and Control of Conducting Polymer Architectures: Structurally Homogeneous Poly(3-alkylthiophenes). *J. Org. Chem.* **1993**, *58*, 904–912.
- (7) Marder, S. R.; Kippelen, B.; Jen, A. K. Y.; Peyghambarian, N. Design and Synthesis of Chromophores and Polymers for Electro-Optic and Photorefractive Applications. *Nature* **1997**, *388*, 845–851.
- (8) Bundgaard, E.; Krebs, F. C. Low Band Gap Polymers for Organic Photovoltaics. *Sol. Energy Mater. Sol. Cells* **2007**, *91*, 954–985.

- (9) Grimsdale, A. C.; Chan, K. L.; Martin, R. E.; Jokisz, P. G.; Holmes, A. B. Synthesis of Light-Emitting Conjugated Polymers for Applications in Electroluminescent Devices. *Chem. Rev.* **2009**, *109*, 897–1091.
- (10) Scherf, U.; List, E. J. W. Semiconducting Polyfluorenes — Towards Reliable Structure–Property Relationships. *Adv. Mater.* **2002**, *14*, 477–487.
- (11) Cheng, Y.-J.; Yang, S.-H.; Hsu, C.-S. Synthesis of Conjugated Polymers for Organic Solar Cell Applications. *Chem. Rev.* **2009**, *109*, 5868–5923.
- (12) Bunz, U. H. F. Poly(aryleneethynylene)s: Syntheses, Properties, Structures, and Applications. *Chem. Rev.* **2000**, *100*, 1605–1644.
- (13) Park, S. H.; Roy, A.; Beaupre, S.; Cho, S.; Coates, N.; Moon, J. S.; Moses, D.; Leclerc, M.; Lee, K.; Heeger, A. J. Bulk Heterojunction Solar Cells with Internal Quantum Efficiency Approaching 100%. *Nat. Photonics* **2009**, *3*, 297–302.
- (14) Roncali, J. Conjugated Poly(thiophenes): Synthesis, Functionalization, and Applications. *Chem. Rev.* **1992**, *92*, 711–738.
- (15) Friend, R. H.; Gymer, R. W.; Holmes, A. B.; Burroughes, J. H.; Marks, R. N.; Taliani, C.; Bradley, D. D. C.; Dos Santos, D. A.; Bredas, J. L.; Logdlund, M.; et al. Electroluminescence in Conjugated Polymers. *Nature* **1999**, *397*, 121–128.
- (16) Scharber, M. C.; Sariciftci, N. S. Efficiency of Bulk-Heterojunction Organic Solar Cells. *Prog. Polym. Sci.* **2013**, *38*, 1929–1940.
- (17) Peet, J.; Kim, J. Y.; Coates, N. E.; Ma, W. L.; Moses, D.; Heeger, A. J.; Bazan, G. C. Efficiency Enhancement in Low-Bandgap Polymer Solar Cells by Processing with Alkane Dithiols. *Nat. Mater.* **2007**, *6*, 497–500.
- (18) Brabec, C. J.; Gowrisanker, S.; Halls, J. J. M.; Laird, D.; Jia, S.; Williams, S. P. Polymer–Fullerene Bulk-Heterojunction Solar Cells. *Adv. Mater.* **2010**, *22*, 3839–3856.
- (19) Brabec, C.; Sariciftci, N.; Hummelen, J. Plastic Solar Cells. *Adv. Funct. Mater.* **2001**, *11*, 15–26.
- (20) Li, G.; Shrotriya, V.; Huang, J.; Yao, Y.; Moriarty, T.; Emery, K.; Yang, Y. High-Efficiency Solution Processable Polymer Photovoltaic Cells by Self-Organization of Polymer Blends. *Nat. Mater.* **2005**, *4*, 864–868.
- (21) Guenes, S.; Neugebauer, H.; Sariciftci, N. S. Conjugated Polymer-Based Organic Solar Cells. *Chem. Rev.* **2007**, *107*, 1324–1338.
- (22) Coakley, K. M.; McGehee, M. D. Conjugated Polymer Photovoltaic Cells. *Chem. Mater.* **2004**, *16*, 4533–4542.
- (23) Dennler, G.; Scharber, M. C.; Brabec, C. J. Polymer–Fullerene Bulk-Heterojunction Solar Cells. *Adv. Mater.* **2009**, *21*, 1323–1338.
- (24) Thompson, B. C.; Fréchet, J. M. J. Organic Photovoltaics — Polymer–Fullerene Composite Solar Cells. *Angew. Chem., Int. Ed.* **2008**, *47*, 58–77.
- (25) Busby, E.; Carroll, E. C.; Chinn, E. M.; Chang, L.; Moule, A. J.; Larsen, D. S. Excited-State Self-Trapping and Ground-State Relaxation Dynamics in Poly(3-hexylthiophene) Resolved with Broadband Pump–Dump–Probe Spectroscopy. *J. Phys. Chem. Lett.* **2011**, *2*, 2764–2769.
- (26) Wells, N. P.; Boudouris, B. W.; Hillmyer, M. A.; Blank, D. A. Intramolecular Exciton Relaxation and Migration Dynamics in Poly(3-hexylthiophene). *J. Phys. Chem. C* **2007**, *111*, 15404–15414.
- (27) Bolinger, J. C.; Traub, M. C.; Adachi, T.; Barbara, P. F. Ultralong-Range Polaron-Induced Quenching of Excitons in Isolated Conjugated Polymers. *Science* **2011**, *331*, 565–567.
- (28) Kobrak, M. N.; Bittner, E. R. A Dynamic Model for Exciton Self-Trapping in Conjugated Polymers. I. Theory. *J. Chem. Phys.* **2000**, *112*, 5399–5409.
- (29) Banerji, N.; Cowan, S.; Vauthey, E.; Heeger, A. J. Ultrafast Relaxation of the Poly(3-hexylthiophene) Emission Spectrum. *J. Phys. Chem. C* **2011**, *115*, 9726–9739.
- (30) Parkinson, P.; Müller, C.; Stingelin, N.; Johnston, M. B.; Herz, L. M. Role of Ultrafast Torsional Relaxation in the Emission from Polythiophene Aggregates. *J. Phys. Chem. Lett.* **2010**, *1*, 2788–2792.
- (31) Bakulin, A. A.; Rao, A.; Pavelyev, V. G.; van Loosdrecht, P. H. M.; Pshenichnikov, M. S.; Niedzialek, D.; Cornil, J.; Beljonne, D.; Friend, R. H. The Role of Driving Energy and Delocalized States for Charge Separation in Organic Semiconductors. *Science* **2012**, *335*, 1340–1344.
- (32) Rozzi, C. A.; Falke, S. M.; Spallanzani, N.; Rubio, A.; Molinari, E.; Brida, D.; Maiuri, M.; Cerullo, G.; Schramm, H.; Christoffers, J.; et al. Quantum Coherence Controls the Charge Separation in a Prototypical Artificial Light-Harvesting System. *Nat. Commun.* **2013**, *4*, 1602.
- (33) Vithanage, D. A.; Devižis, A.; Abramavičius, V.; Infahsaeng, Y.; Abramavičius, D.; MacKenzie, R. C. I.; Keivanidis, P. E.; Yartsev, A.; Hertel, D.; Nelson, J.; et al. Visualizing Charge Separation in Bulk Heterojunction Organic Solar Cells. *Nat. Commun.* **2013**, *4*, 2334.
- (34) Provencher, F.; Bérubé, N.; Parker, A. W.; Greetham, G. M.; Towrie, M.; Hellmann, C.; Côté, M.; Stingelin, N.; Silva, C.; Hayes, S. C. Direct Observation of Ultrafast Long-Range Charge Separation at Polymer–Fullerene Heterojunctions. *Nat. Commun.* **2014**, *5*, 4288.
- (35) Gélinas, S.; Rao, A.; Kumar, A.; Smith, S. L.; Chin, A. W.; Clark, J.; van der Poll, T. S.; Bazan, G. C.; Friend, R. H. Ultrafast Long-Range Charge Separation in Organic Semiconductor Photovoltaic Diodes. *Science* **2014**, *343*, 512–516.
- (36) Kaake, L. G.; Moses, D.; Heeger, A. J. Coherence and Uncertainty in Nanostructured Organic Photovoltaics. *J. Phys. Chem. Lett.* **2013**, *4*, 2264–2268.
- (37) Grancini, G.; Maiuri, M.; Fazzi, D.; Petrozza, A.; Egelhaaf, H.-J.; Brida, D.; Cerullo, G.; Lanzani, G. Hot Exciton Dissociation in Polymer Solar Cells. *Nat. Mater.* **2013**, *12*, 29–33.
- (38) Falke, S. M.; Rozzi, C. A.; Brida, D.; Maiuri, M.; Amato, M.; Sommer, E.; De Sio, A.; Rubio, A.; Cerullo, G.; Molinari, E.; et al. Coherent Ultrafast Charge Transfer in an Organic Photovoltaic Blend. *Science* **2014**, *344*, 1001–1005.
- (39) Cabanillas-Gonzalez, J.; Grancini, G.; Lanzani, G. Pump–Probe Spectroscopy in Organic Semiconductors: Monitoring Fundamental Processes of Relevance in Optoelectronics. *Adv. Mater.* **2011**, *23*, 5468–5485.
- (40) Cowan, S. R.; Banerji, N.; Leong, W. L.; Heeger, A. J. Charge Formation, Recombination, and Sweep-Out Dynamics in Organic Solar Cells. *Adv. Funct. Mater.* **2012**, *22*, 1116–1128.
- (41) Lakhwani, G.; Rao, A.; Friend, R. H. Bimolecular Recombination in Organic Photovoltaics. *Annu. Rev. Phys. Chem.* **2014**, *65*, 557–581.
- (42) Chen, K.; Barker, A. J.; Reish, M. E.; Gordon, K. C.; Hodgkiss, J. M. Broadband Ultrafast Photoluminescence Spectroscopy Resolves Charge Photogeneration via Delocalized Hot Excitons in Polymer–Fullerene Photovoltaic Blends. *J. Am. Chem. Soc.* **2013**, *135*, 18502–18512.
- (43) Hao, X.-T.; Chan, N. Y.; Dunstan, D. E.; Smith, T. A. Conformational Changes and Photophysical Behavior in Poly[2-methoxy-5-(2'-ethyl-hexyloxy)-1,4-phenylene vinylene] Thin Films Cast under an Electric Field. *J. Phys. Chem. C* **2009**, *113*, 11657–11661.
- (44) Clark, J.; Nelson, T.; Tretiak, S.; Cirri, G.; Lanzani, G. Femtosecond Torsional Relaxation. *Nat. Phys.* **2012**, *8*, 225–231.
- (45) Tapping, P. C.; Kee, T. W. Optical Pumping of Poly(3-hexylthiophene) Singlet Excitons Induces Charge Carrier Generation. *J. Phys. Chem. Lett.* **2014**, *5*, 1040–1047.
- (46) Gaab, K. M.; Bardeen, C. J. Anomalous Exciton Diffusion in the Conjugated Polymer MEH-PPV Measured Using a Three-Pulse Pump–Dump–Probe Anisotropy Experiment. *J. Phys. Chem. A* **2004**, *108*, 10801–10806.
- (47) van Wilderen, L. J. G. W.; Clark, I. P.; Towrie, M.; van Thor, J. J. Mid-Infrared Picosecond Pump–Dump–Probe and Pump–Repump–Probe Experiments to Resolve a Ground-State Intermediate in Cyanobacterial Phytochrome Cph1. *J. Phys. Chem. B* **2009**, *113*, 16354–16364.
- (48) Fitzpatrick, A. E.; Lincoln, C. N.; van Wilderen, L. J. G. W.; van Thor, J. J. Pump–Dump–Probe and Pump–Repump–Probe Ultrafast Spectroscopy Resolves Cross Section of an Early Ground State

Intermediate and Stimulated Emission in the Photoreactions of the Pr Ground State of the Cyanobacterial Phytochrome Cph1. *J. Phys. Chem. B* **2012**, *116*, 1077–1088.

(49) Gadermaier, C.; Cerullo, G.; Sansone, G.; Leising, G.; Scherf, U.; Lanzani, G. Time-Resolved Charge Carrier Generation from Higher Lying Excited States in Conjugated Polymers. *Phys. Rev. Lett.* **2002**, *89*, 117402.

(50) Maroncelli, M. Computer-Simulations of Solvation Dynamics In Acetonitrile. *J. Chem. Phys.* **1991**, *94*, 2084–2103.

(51) Rosenthal, S. J.; Xie, X.; Du, M.; Fleming, G. R. Femtosecond Solvation Dynamics in Acetonitrile: Observation of the Inertial Contribution to the Solvent Response. *J. Chem. Phys.* **1991**, *95*, 4715–4718.

(52) Jimenez, R.; Fleming, G. R.; Kumar, P. V.; Maroncelli, M. Femtosecond Solvation Dynamics of Water. *Nature* **1994**, *369*, 471–473.

(53) Bardeen, C. J.; Wang, Q.; Shank, C. V. Femtosecond Chirped Pulse Excitation of Vibrational Wave Packets in LD690 and Bacteriorhodopsin. *J. Phys. Chem. A* **1998**, *102*, 2759–2766.

(54) Gai, F.; McDonald, J. C.; Anfinrud, P. A. Pump–Dump–Probe Spectroscopy of Bacteriorhodopsin: Evidence for a Near-IR Excited State Absorbance. *J. Am. Chem. Soc.* **1997**, *119*, 6201–6202.

(55) Larsen, D. S.; Vengris, M.; van Stokkum, I. H. M.; van der Horst, M. A.; de Weerd, F. L.; Hellingwerf, K. J.; van Grondelle, R. Photoisomerization and Photoionization of the Photoactive Yellow Protein Chromophore in Solution. *Biophys. J.* **2004**, *86*, 2538–2550.

(56) van Thor, J. J.; Zanetti, G.; Ronayne, K. L.; Towrie, M. Structural Events in the Photocycle of Green Fluorescent Protein. *J. Phys. Chem. B* **2005**, *109*, 16099–16108.

(57) van Amerongen, H.; van Grondelle, R.; Valkunas, L. *Photosynthetic Excitons*; World Scientific Publishing: River Edge, NJ, 2000.

(58) Yan, M.; Rothberg, L. J.; Kwock, E. W.; Miller, T. M. Interchain Excitations in Conjugated Polymers. *Phys. Rev. Lett.* **1995**, *75*, 1992–1995.

(59) Hsu, J. W. P.; Yan, M.; Jedju, T. M.; Rothberg, L. J.; Hsieh, B. R. Assignment of the Picosecond Photoinduced Absorption in Phenylene Vinylene Polymers. *Phys. Rev. B* **1994**, *49*, 712–715.

(60) Deibel, C.; Strobel, T.; Dyakonov, V. Origin of the Efficient Polaron-Pair Dissociation in Polymer–Fullerene Blends. *Phys. Rev. Lett.* **2009**, *103*, 036402.

(61) Søndergaard, R.; Hösel, M.; Angmo, D.; Larsen-Olsen, T. T.; Krebs, F. C. Roll-to-Roll Fabrication of Polymer Solar Cells. *Mater. Today* **2012**, *15*, 36–49.

(62) Hoke, E. T.; Vandewal, K.; Bartelt, J. A.; Mateker, W. R.; Douglas, J. D.; Noriega, R.; Graham, K. R.; Fréchet, J. M. J.; Salleo, A.; McGehee, M. D. Recombination in Polymer:Fullerene Solar Cells with Open-Circuit Voltages Approaching and Exceeding 1.0 V. *Adv. Energy Mater.* **2013**, *3*, 220–230.

(63) Vandewal, K.; Albrecht, S.; Hoke, E. T.; Graham, K. R.; Widmer, J.; Douglas, J. D.; Schubert, M.; Mateker, W. R.; Bloking, J. T.; Burkhard, G. F.; et al. Efficient Charge Generation by Relaxed Charge-Transfer States at Organic Interfaces. *Nat. Mater.* **2014**, *13*, 63–68.

(64) Westenhoff, S.; Daniel, C.; Friend, R. H.; Silva, C.; Sundström, V.; Yartsev, A. Exciton Migration in a Polythiophene: Probing the Spatial and Energy Domain by Line-Dipole Förster-Type Energy Transfer. *J. Chem. Phys.* **2005**, *122*, 094903.

(65) Kukura, P.; McCamant, D. W.; Mathies, R. A. Femtosecond Stimulated Raman Spectroscopy. *Annu. Rev. Phys. Chem.* **2007**, *58*, 461–488.

(66) Smith, M. B.; Michl, J. Recent Advances in Singlet Fission. *Annu. Rev. Phys. Chem.* **2013**, *64*, 361–386.

(67) Smith, M. B.; Michl, J. Singlet Fission. *Chem. Rev.* **2010**, *110*, 6891–6936.

(68) Shockley, W.; Queisser, H. J. Detailed Balance Limit of Efficiency of p–n Junction Solar Cells. *J. Appl. Phys.* **1961**, *32*, 510–519.

(69) Hanna, M. C.; Nozik, A. J. Solar Conversion Efficiency of Photovoltaic and Photoelectrolysis Cells with Carrier Multiplication Absorbers. *J. Appl. Phys.* **2006**, *100*, 074510.

(70) Larsen, D. S.; Papagiannakis, E.; van Stokkum, I. H.; Vengris, M.; Kennis, J. T.; van Grondelle, R. Excited State Dynamics of β -Carotene Explored with Dispersed Multi-Pulse Transient Absorption. *Chem. Phys. Lett.* **2003**, *381*, 733–742.

(71) Austin, R. H.; Baker, G. L.; Etemad, S.; Thompson, R. Magnetic Field Effects on Triplet Exciton Fission and Fusion in a Polydiacetylene. *J. Chem. Phys.* **1989**, *90*, 6642–6646.

(72) Bittner, E. R.; Lankevich, V.; Gelinas, S.; Rao, A.; Ginger, D. A.; Friend, R. H. How Disorder Controls the Kinetics of Triplet Charge Recombination in Semiconducting Organic Polymer Photovoltaics. *Phys. Chem. Chem. Phys.* **2014**, DOI: 10.1039/C4CP01776E.

(73) Rao, A.; Chow, P. C. Y.; Gelinas, S.; Schlenker, C. W.; Li, C.-Z.; Yip, H.-L.; Jen, A. K.-Y.; Ginger, D. S.; Friend, R. H. The Role of Spin in the Kinetic Control of Recombination in Organic Photovoltaics. *Nature* **2013**, *500*, 435–439.

(74) Grumstrup, E. M.; Johnson, J. C.; Damrauer, N. H. Enhanced Triplet Formation in Polycrystalline Tetracene Films by Femtosecond Optical-Pulse Shaping. *Phys. Rev. Lett.* **2010**, *105*, 257403.

(75) Hodgkiss, J. M.; Albert-Seifried, S.; Rao, A.; Barker, A. J.; Campbell, A. R.; Marsh, R. A.; Friend, R. H. Exciton–Charge Annihilation in Organic Semiconductor Films. *Adv. Funct. Mater.* **2012**, *22*, 1567–1577.